ELFE AT CERN: A 25 GeV C.W. ELECTRON ACCELERATOR

E. Keil, CERN, Geneva, Switzerland

Abstract

ELFE at CERN is the study of a quasi continuous electron accelerator that accelerates an average current of about 0.1 mA to 25 GeV. A polarized electron beam is injected into either a racetrack microtron or into a first recirculating linear accelerator and accelerated to 800 MeV. The acceleration from there to 25 GeV is achieved in a second recirculating linear accelerator. The beam passes seven times through super-conducting RF cavities that were previously used in LEP2, and gains about 3.5 GeV on each pass. The hadronic physics and machine aspects have been studied by a joint NuPECC-CERN Study Group. This paper reports on the findings of the machine study. Several of the following topics will be covered: Beam dynamics in a recirculating linear accelerator with a super-conducting RF system, vacuum, construction in the North Area of the SPS, experimental areas, manpower, cost and construction schedule.

1 INTRODUCTION

ELFE stands for **E**lectron **L**aboratory **F**or **E**urope. It is a quasi continuous electron accelerator similar to CEBAF.ELFE at CERN is its third manifestation. The earlier ones are ELFE on a green site in October 1993 [1], and ELFE at DESY in 1997 [2]. ELFE at CERN is one of the possibilities for recycling the LEP super-conducting 3.5 GeV relativistic c.w. RF system once LEP is shut down. Figure 1 shows one of the four-cell cavities. The ELFE at CERN study was set up jointly by NuPECC (Nuclear Physics European Coordinating Committee) and CERN. The conceptual machine design report was published in December 1999 [3]. Reports on hadronic physics with ELFE were published in 1992 [4] and 1996 [5]. New reports on the hadronic physics and the detectors at ELFE are still to come.

Table 1: Nominal ELFE Beam Parameters

Top energy	25	GeV
Beam current on target	100	μA
Injection energy	0.8	GeV
Number of passes	7	
Energy gain per pass	3.5	GeV
Relative rms momentum spread	$\leq 10^{-3}$	
Emittance at top energy	≤ 30	nm
Bunch repetition time on target	2.8	ns

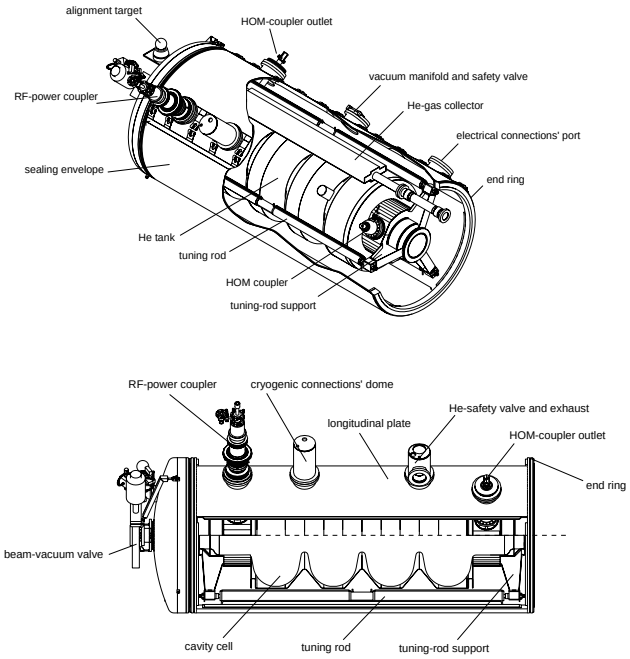

Figure 1: Two views of a four-cell cavity of the LEP superconducting RF system. Four such cells form a module, and 72 modules the complete system.

2 NOMINAL ELFE BEAM PARAMETERS

Table 1 shows the nominal ELFE beam parameters. Acceleration to an energy of approximately 25 GeV is about the maximum that we can achieve with the 3.5 GV from the LEP RF system and 7 passes. Proposing 7 passes and associated spreaders and combiners is a challenge and will be discussed in Section 3.3. The beam current meets the specification. It is about the maximum that is expected to be put on a target in an experimental hall equipped with a spectrometer covering a small solid angle. The beam current on a target surrounded by a 4π detector is much smaller. The ongoing physics study considers just one detector. The specified emittance imposes an upper limit on the quantum excitation in the arcs, spreaders and combiners, and hence upper limits on the horizontal and vertical dispersions D_x and D_y, as well as a lower limit on the bending radius ρ in the arcs. The momentum spread should be small compared to the π mass. This condition imposes again a lower limit on the bending radius, as well as a tight upper limit on bunch length σ_s because of the RF wave form in the neighbourhood of the crest. How the ELFE arcs, spreader and combiner meet these requirements is dis-

cussed in Sections 3.4 to 3.6. A smaller momentum spread would be better for polarisation, but it would need an even larger bending radius in the arcs. The bunch repetition frequency is determined by the frequency of the LEP RF system, 352 MHz.

3 OPTICS OF ELFE

In this chapter, I discuss the optical design of ELFE. First, I present how ELFE is split into optical modules. Then I explain my design approach that consists of a combination of symbolic and numerical codes, which I use for the geometrical design of the spreaders and the optical design of the arcs. Finally, I introduce the notion of tracking 10^4 to 10^5 particles, and use it to determine the energy spread and emittances of the beam at the exit of ELFE, caused by quantum excitation.

3.1 Optical Modules

Figure 2 shows the optical modules of ELFE. A polarized electron beam is injected into either a racetrack microtron or into a first recirculating linear accelerator and accelerated to 800 MeV. The electrons are then injected into the upstream end of the 3.5 GeV linac which they pass seven times. The spreader at the downstream end of the linac feeds the beams into six vertically stacked arcs. The arcs are isochronous and derived from double bend achromats. Six matching sections match the beams between the arcs and six identical vertically stacked return lines. Six matching sections which at the downstream end of the return lines which are mirror images of those at the upstream ends match the beams into six arcs which are identical to the other six arcs. The combiner feeds the beams into the linac. It is geometrically identical to the spreader, but optically different. Exit lines take the beam to the experimental halls. The major and minor axes are 1.8 km and 0.3 km, respectively.

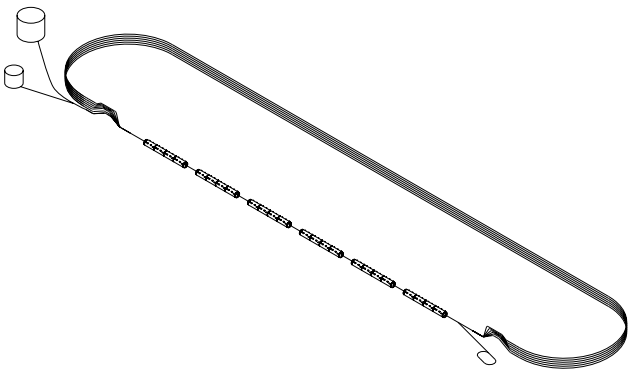

Figure 2: Layout of ELFE, showing the optical modules. The injector is in the lower right corner, the experimental halls in the upper left corner.

An alternative to the ELFE design would be a machine with two linear accelerators of half the length of the present one. One would save on the linear accelerator tunnel and on the return line, but would need an extra spreader and an extra combiner with seven beam lines instead of six and the added quantum excitation in the vertical direction, and seven vertically stacked arcs at the downstream end of the first linear accelerator. Estimates show that the cost savings are marginal.

3.2 Automated Design Approach

For parameter searches and the study of consequences of my input choices, I have developed a technique that combines two styles of calculations [6]:

- Approximate calculations in thin-element approximation with *Mathematica* or a similar product, but not in languages like FORTRAN, C or C++
- Precise calculations, including finite elements, matching, edge effects, tracking, etc., with MAD [7] or a similar product

The technique includes selecting and applying rules. Examples of rules are " The dipole field is $B = 1$ T " or " The quadrupole field at the edge of the as yet unknown aperture is $B = 2$ T ". Applying rules like "The number of achromat pairs in the ELFE arcs is an integer" and calculating bending angles from that number ensures that the ELFE geometry is always correct. It is surprisingly fast and easy to get a feeling for the effects of various choices on the ELFE parameters, only with the approximate calculations in *Mathematica*. The precise calculations with MAD only start when one has settled for a likely set of choices.

The accelerator physics is embedded in *Mathematica* notebooks and packages. Typically, the accelerator physics, e.g. related to FODO cells, RF systems, synchrotron radiation, or collective effects, is assembled in packages that are written such that they work for any kind of particle. In fact, I have used some of these packages for circular colliders of e^+e^- and protons, for recirculating linear accelerators for electrons and muons, and for muon storage rings. The functions in the packages are invoked by notebooks that are related to machines. *Mathematica* writes short files that are read by MAD, and used as initial guesses for matching. This is made easy by the fact that MAD can read expressions. The power of this approach is not in individual ingredients, e.g. the β-function in a FODO lattice, but in their combination.

3.3 Spreader Geometry

Figure 3 shows the geometry of the spreader that feeds the beams from the linear accelerator into six vertically stacked arcs and the exit line towards the experimental halls. The linear accelerator is at the left, arcs at the right. The bending angles in the vertical dipole at the left edge are $\propto 1/E$. The second series of dipoles are staggered along the horizontal axis in order to make the vertical separation between the beam lines as small as possible. The scale of the bending angles is fixed by the requirement that the vertical dis-

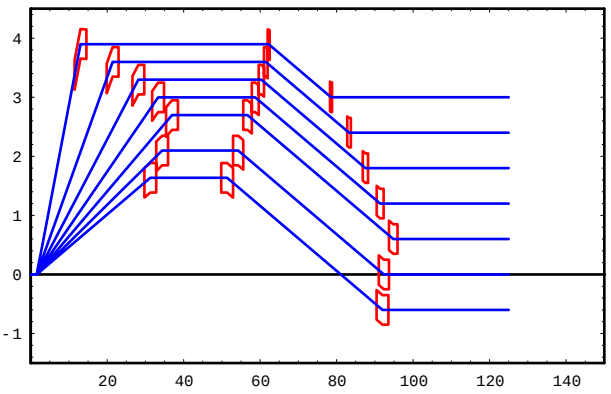

Figure 3: Spreader geometry. The distances are in metres.

tance between the lowest two lines $\ell(\varphi_2 - \varphi_1)$ is larger than or equal to the dipole half height. Here ℓ is the distance between the first and second dipoles along the spreader. The larger the number of passes, the smaller is the relative difference between the energies of the last and the last-but-one pass, ans the larger is the bending angle φ_1 for the last pass. Hence, the height of spreader and combiner increases rapidly with the number of passes. The number proposed for ELFE, seven, is close to the limit. The third series of dipoles is again staggered along the horizontal direction. The downwards lines are parallel to each other. The separations in the spreader and the arcs are prescribed. All these statements are formulated as rules in *Mathematica*.

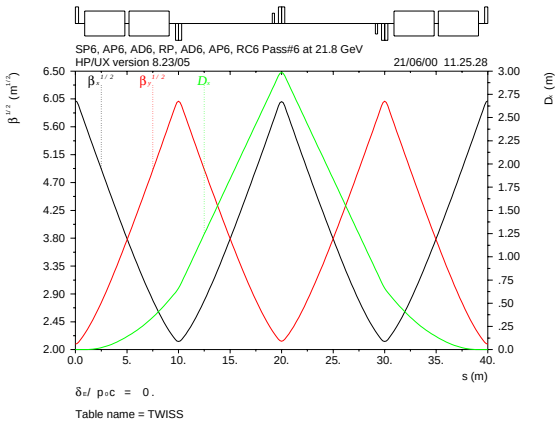

Figure 4: Typical double bend achromat

3.4 *Arc Lattice*

The lattice of the arcs is derived from the double bend achromat in Figure 4. It was proposed for the synchrotron light source SOLEIL [8], has dipoles in only 50% of the available spaces, and equal and opposite quadrupole gradients. Their values are adjusted such that $D'_x = 0$ at the centre, when one starts with $D_x = D'_x = 0$ at the entrance. It follows from symmetry that $D_x = D'_x = 0$ also at the end. This fit with one condition and one constraint has a unique solution for quadrupole strength, β-functions and D_x. The corresponding thin-element formulae are embedded in *Mathematica*. The isochronism in ELFE is achieved by arranging achromats in pairs and adjusting D_x at the centre of a pair. This adjustment includes the contribution of spreader and combiner to the anisochronism R_{56}. Figure 5 shows the layout and optical functions of a pair of achromats at 4.3 GeV. The negative contribution of spreader and combiner to R_{56} are compensated by a positive contribution of the arcs which is obtained by the positive dispersion D_x in the dipoles near the centre.

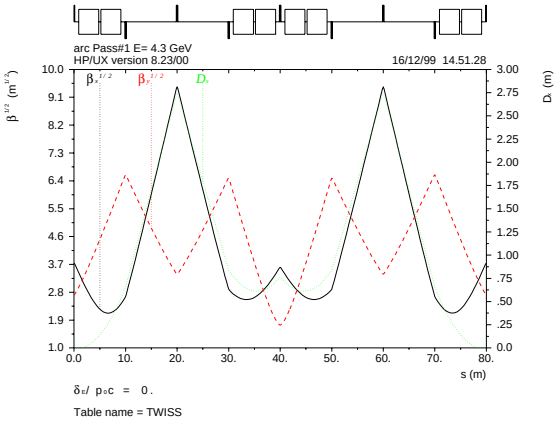

Figure 5: Layout and optical functions of the achromat pairs at 4.3 GeV

3.5 *Multi-Particle Tracking*

On a typical server, tracking 10^4 to 10^5 particles through ELFE takes a few minutes. The limit on the number of particles is given by the space allocated to the particle coordinates in the tracking program, and no longer by computer time. This makes it possible to observe particle distribution functions. Figures 6 to 9 show examples of distribution functions at the end of the 6-th pass for point-like bunches starting at the beginning of the 6-th pass, obtained by tracking 30000 particles through spreader, arc, matching section, return line, reflected matching section, arc and combiner. Specifically, Figures 6 and 7 show the quantum excitation of the horizontal betatron motion. Figure 8 shows the longitudinal beam profile. The average particle arrives a little later than the reference particle. The spread in ct is presumably caused by higher order terms in the anisochronism. Figure 9 shows the distribution in the relative momentum error $\delta p/p$. The mean offset measures the synchrotron radiation loss, the standard deviation the quantum excitation on the sixth pass.

Using a post-processor [9] to the tracking program MAD [7], I find the mean values of the particle coordinates $\bar{x}$, $\bar{x}'$, $\bar{y}$, $\bar{y}'$, $\bar{t}$, $\bar{\delta}$, and derive the horizontal emittance ϵ_x by

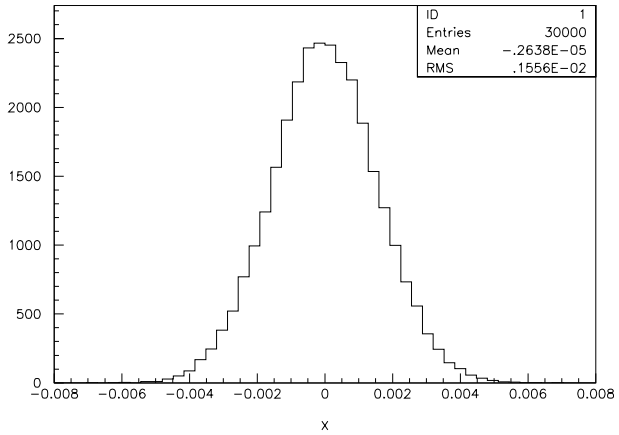

Figure 6: Horizontal beam size x in m at $\beta_x = 200$ m

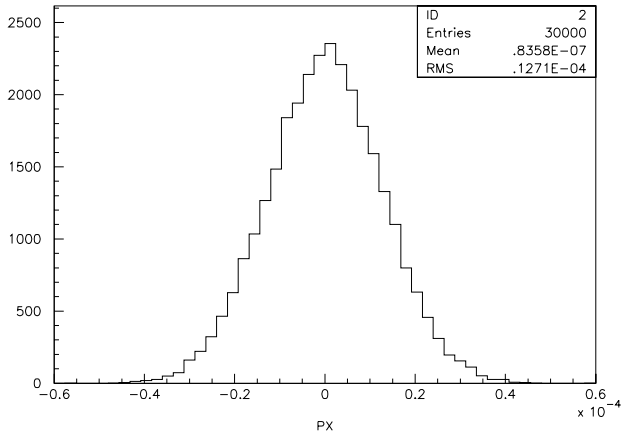

Figure 7: Horizontal beam divergence x' in r at $\alpha_x = 0$ and $\beta_x = 200$ m

generalizing from [10]:

$$\epsilon_x = \sqrt{\langle (x-\bar{x})^2 \rangle \langle (x'-\bar{x}')^2 \rangle - \langle (x-\bar{x})^2 (x'-\bar{x}')^2 \rangle}$$

Here the angular brackets $\langle \ldots \rangle$ indicate means. The equations for ϵ_y and ϵ_t are similar.

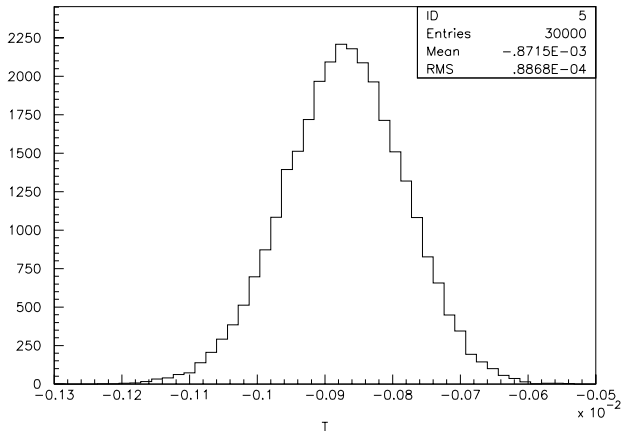

Figure 8: Bunch length ct in m

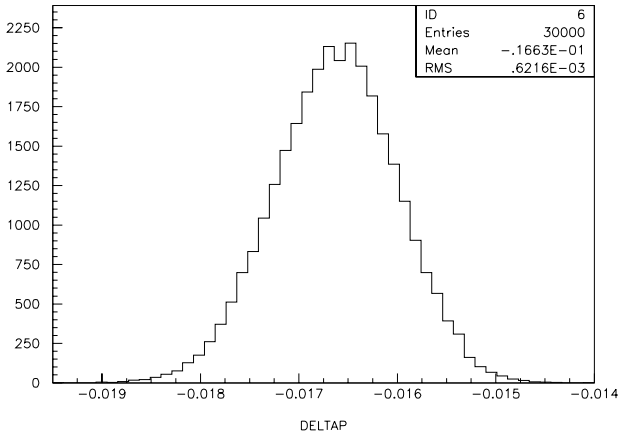

Figure 9: Relative energy error $\delta p/p$

Table 2: Nominal energy E, synchrotron radiation loss/pass U, accumulated relative energy spread σ_e in units of 10^{-3}, horizontal emittance ϵ_x in nm and vertical emittance ϵ_y in nm for the seven passes through ELFE. The last line shows the parameters at the exit.

No.	E/GeV	U/MeV	$\sigma_e/10^{-3}$	ϵ_x/nm	ϵ_y/nm
1	4.3	1.28	0.2780	0.0032	0.723
2	7.8	8.29	0.3161	0.0891	2.965
3	11.3	30.59	0.3555	0.722	4.337
4	14.8	82.92	0.4292	3.247	6.806
5	18.3	185.14	0.5733	10.58	10.33
6	21.8	362.46	0.8035	27.84	14.44
7	25.3	22.51	0.7354	23.96	18.83
Tot.	24.6	697.40	0.7354	23.96	18.83

3.6 Emittance and Energy Spread

In order to obtain the emittances and the energy spread at the exit of ELFE, I track 30000 particles with quantum excitation through one pass at a time. I launch the particles at the entrance of the first pass with $x = x' = y = y' = \delta p/p = 0$, neglecting the emittance and energy spread of the injected beam, and a bunch length $\sigma_s = 3$ mm. This approximation is well justified [3]. Between passes, I reset the mean values of the particle coordinates $\bar{x}$, $\bar{x}'$, $\bar{y}$, $\bar{y}'$, $\bar{t}$, $\bar{\delta}$ to zero, as one would do when setting up ELFE. I observe the synchrotron radiation loss U/pass, the accumulated relative energy spread σ_e, and the accumulated emittances ϵ_x and ϵ_y. Table 2 shows the results. Only ϵ_x scales as naïvely expected. The other quantities are affected by the spreader and the combiner. On the seventh pass, which only includes a spreader but no arcs, U is small. The relative momentum spread σ_e and the unnormalized emittance ϵ_x become smaller, since E actually increases. Only ϵ_y increases because of the vertical quantum excitation in the spreader. The total energy loss due to synchrotron radiation is almost 700 MeV, resulting in a maximum energy 24.6 GeV, somewhat less than the nominal 25 GeV. Energy

spread and the emittances are below the values specified in Table 1.

4 ELFE ON CERN SITE

Figure 10 shows where ELFE might be located in the North area of the SPS. The existing ECN3 hall might perhaps be used as one of the experimental halls of ELFE.

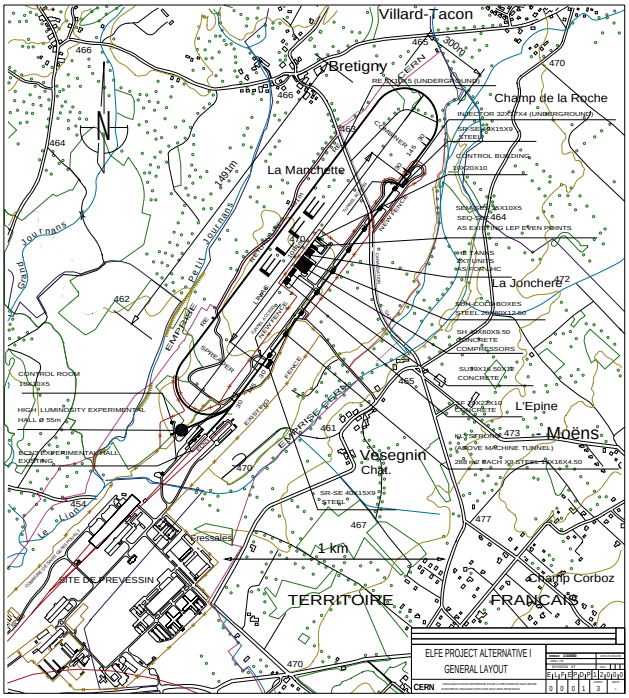

Figure 10: ELFE on CERN Site. The laboratory and office buildings of the Prevessin site are shown in the lower left corner.

5 CONCLUSIONS

ELFE at CERN is a 25 GeV quasi continuous electron accelerator with a beam power of 2.5 MW. It would use the super-conducting LEP RF cavities. The authors of the ELFE study think that it meets the design specifications and will work. ELFE fits on the CERN site and can be built in about 6.5 years from project approval. The capital expenditure for ELFE is about 366 MCHF, to be found outside the CERN budget. More detailed cost and manpower estimates are available [3].

The optical design process can be automated to a large extent by having *Mathematica* and MAD, or similar products, communicate with each other by files. Accurate beam parameters can be found by tracking 10^4 to 10^5 particles, and processing the results automatically. I have pushed the automation further in more recent applications, e.g. muon recirculating linear accelerators and muon storage rings for a neutrino factory.

REFERENCES

[1] Electron Laboratory for Europe, Accelerator technical proposal, "Blue book", J.-M. De Conto (Ed.), Institut des Sciences Nucléaires de Grenoble, RME02 (October 1993).

[2] R. Brinkmann *et al.*, "The Machine Project for ELFE at DESY," *Nucl. Phys.* **A622** (1997) 187c–224c.

[3] B. Aune, J. Aysto, J.-L. Baldy, H. Burkhardt (Ed.), F. Bradamante, E. Cennini, S. Claudet, C. Détraz, E. De Sanctis, H. Fonvieille, H. Frischholz, S. Galès, M. Garçon, G. Gemme, R. Genand, G. Geschonke, P. Grafstrom, N. Hilleret, M. Hoffmann, P. Hoyer, K. Hübner, D. Husmann, J. Inigo-Golfin, M. Jablonka, K.H. Kaiser, E. Keil, G.-E. Körner, S. Kox, J.-M. Laget, J. Lindroos, J. Martino, Y. Muttoni, R. Parodi, J. Payet, J. Pedersen, G. Ricco, M. Sassowsky, H. Schmickler, G. Smirnov, G.R. Stevenson, I. Sick, F. Tazzioli, A. Tkatchenko, R. Van de Vyver, Th. Walcher, ELFE at CERN – Conceptual Design Report, CERN 99/10 (1999)

[4] The ELFE Project: an Electron Laboratory for Europe, Proc. of Mainz workshop (Oct. 92) edited by J. Arvieux and E. De Sanctis, Editrice Compositori, Bologna 1993.

[5] Prospects of hadron and quark physics with electromagnetic probes, Proc. of Saint-Malo workshop (Sept. 96), edited by N. D'Hose et al., Nucl. Phys. **A622** (1997) 1c-389c.

[6] E. Keil, Muon Storage Rings Design with Simple Mathematica Packages, CERN-SL-99-053-AP (1999).

[7] H. Grote and F.C. Iselin, The MAD Program, Version 8.16, User's Reference Manual, CERN SL/90-13 (AP) Rev.4 (1995).

[8] P. Nghiem et al., Optics for SOLEIL at 2.5 GeV, Proc. Particle Accel. Conf. (Vancouver 1997) 1406.

[9] E. Keil, Histograms of MAD Tracking results, CERN-NUFACT-NOTE-12, CERN-SL-NOTE-99-061-AP (Dec 1999).

[10] A.W. Chao and M. Tigner (eds.), Handbook of Accelerator Physics and Engineering (World Scientific, Singapore 1999) 50.